



# Magnetic Resonance Venography Findings of Obstructed Hepatic Veins and the Inferior Vena Cava in Patients with Budd-Chiari Syndrome

Ru-Xin Song, MM<sup>1</sup>, Shi-Feng Cai, MD<sup>2</sup>, Shuang Ma, MB<sup>3</sup>, Zhi-Ling Liu, MD<sup>2</sup>, Yong-Hao Gai, MD, PhD<sup>1</sup>, Chun-Qing Zhang, MD<sup>4</sup>, Guang-Chuan Wang, MD<sup>4</sup>

Departments of <sup>1</sup>Ultrasound, <sup>2</sup>Radiology, and <sup>4</sup>Gastroenterology, Shandong Provincial Hospital Affiliated to Shandong University, Ji'nan 250021, China; <sup>3</sup>Department of Ultrasound, Fifth Hospital of Jinan, Ji'nan 250000, China

**Objective:** This study aimed to illustrate the magnetic resonance venography (MRV) manifestations of obstructed hepatic veins (HVs), the inferior vena cava (IVC), and accessory hepatic veins (AHVs) in patients with Budd-Chiari syndrome (BCS) and to evaluate the visualization capacity of MRV in the diagnosis of BCS.

**Materials and Methods:** Fifty-two patients with chronic BCS were included in this study. All patients were examined via MRV performed with a 3T system following injections of gadolinium-diethylene triamine pentaacetic acid (Gd-DTPA) or Gd-ethoxibenzyl-DTPA. HV and IVC lesions were classified, and their characteristics were described. HV cord-like occlusions detected via MRV were compared using ultrasonography (US). Digital subtraction angiography (DSA) was performed as a contrast in the MRV detection of IVC lesions. The HVs draining collaterals, mainly AHVs, were carefully observed. HV lesions were classified as segmental stenosis, segmental occlusion, membranous stenosis, membranous occlusion, cord-like occlusion, or non-visualized. Except for patent IVCs, IVC lesions were classified as segmental occlusion, segmental stenosis, membranous occlusion, membranous stenosis, and hepatomegaly-induced stenosis.

**Results:** All patients (52/52, 100%) showed HV lesions of different degrees. MRV was inferior to US in detecting cord-like occlusions (6 vs. 19,  $\chi^2 = 11.077$ ,  $p < 0.001$ ). Dilated AHVs, including 50 (50/52, 96.2%) caudate lobe veins and 37 (37/52, 71.2%) inferior HV and AHV lesions, were well-detected. There were no significant differences in detecting segmental lesions and thrombosis between MRV and DSA ( $\chi^2 = 0.000$ ,  $p_1 = 1.000$ ,  $p_2 = 1.000$ ). The capacity of MRV to detect membranous lesions was inferior to that of DSA (7 vs. 15,  $\chi^2 = 6.125$ ,  $p = 0.013$ ).

**Conclusion:** In patients with BCS, MRV can clearly display the lesions in HVs and the IVC, as well as in AHVs, and it has diagnostic and therapeutic value.

**Keywords:** Budd-Chiari syndrome; MOVIC; Magnetic resonance imaging; Venography; Angiography; Inferior vena cava; Hepatic vein

## INTRODUCTION

Budd-Chiari syndrome (BCS) is defined as portal hypertension with hepatomegaly caused by hepatic venous outflow obstruction at the level of the major hepatic veins

(HVs) or the retrohepatic segment of the inferior vena cava (IVC) (1, 2). This rare disease has a high prevalence in less-developed regions and is more common in rural areas, where sanitation and medical facilities are insufficient and social conditions facilitate the spread of disease. Unlike

Received June 5, 2017; accepted after revision October 2, 2017.

This study was supported by the Shandong Provincial Science and Technology Development Project Foundation of China (nos. 2013GSF11827 and 2015GSF118012) and the Health Care and Family Planning Technology Development Plans of Shandong Province (nos. 2013WS0108).

**Corresponding author:** Yong-Hao Gai, MD, PhD, Department of Ultrasound, Shandong Provincial Hospital Affiliated to Shandong University, 324 Jingwu Road, Ji'nan 250021, China.

• Tel: (86) 15168889066 • Fax: (86) 0531-68773689 • E-mail: yhgaiusdoc@163.com

This is an Open Access article distributed under the terms of the Creative Commons Attribution Non-Commercial License (<http://creativecommons.org/licenses/by-nc/4.0>) which permits unrestricted non-commercial use, distribution, and reproduction in any medium, provided the original work is properly cited.

in the Western world, where acute BCS is the main form of the disease, in China and Japan, patients with chronic BCS represent the majority of cases (3). The pathogenesis of venous lesions indicates that obstructions can be located in all HVs, and this involvement usually occurs asynchronously and progresses at variable speeds (4). Imaging can reveal obstructions in HVs and the IVC, including the site and extent of the obstructions, as well as the draining conditions of emerging collateral pathways; therefore, imaging is an important procedure for diagnosing BCS. The value of ultrasound and angiography in diagnosing BCS has been well studied and confirmed. This study aimed to illustrate the types of venous involvement in patients with BCS using magnetic resonance venography (MRV) and to evaluate the manifestations displayed by MRV and the value of MRV in diagnosing BCS.

## MATERIALS AND METHODS

### Patients

Institutional Review Board approval was obtained for this study, and written informed consent was obtained from all patients. This study was based on MRV data obtained between January 2012 and November 2015 from 52 patients with chronic BCS, including 24 male (age range, 29–61 years; mean age,  $52.0 \pm 9.7$  years) and 28 female (age range, 29–63 years; mean age,  $47.6 \pm 10.1$  years) patients. Diagnoses of BCS were confirmed via digital subtraction angiography (DSA) and ultrasonography (US). In all patients, the time from the first clinical symptom to diagnosis ranged from 2 weeks to 24 years. The main clinical symptoms included right upper abdominal distension, abdominal wall varicosis, edema and/or varicosis of both lower extremities. Patients in whom BCS was secondary to compression of the HV by a tumor or malignant cell embolism were excluded.

This study was approved by the Ethics Committee of the Shandong Provincial Hospital affiliated to Shandong University (Ji'nan, China), and written informed consent was obtained from all patients.

### MRV Technique

All magnetic resonance (MR) examinations were performed with a 3T system (Magnetom Verio; Siemens®, Munich, Germany) equipped with an 8-channel abdominal phased-array surface coil for signal reception. Abdominal transverse conventional sequences, pre-contrast three-dimensional (3D) fat-saturated T1-weighted sequences (volume interpolated

body examination; Siemens®) and coronal mask scans were initially performed. Transverse contrast-enhanced 3D-volume-interpolated body examination (3D-VIBE T1WI) sequences of the upper abdomen were acquired during suspended respiration 20 seconds after contrast injection, followed by a large-area 3D contrast-enhanced scan for venous vessels. For each patient, the images covered the region from the hilum to the iliac crest and from the abdominal wall to the vertebral trailing edge. FL3D image scanning was performed in the coronal plane at 55, 90, and 120 seconds after contrast injection, allowing sufficient time intervals for breathing. The scanning conditions were the same as for the previous scan. The technical parameters were as follows: repetition time, 2.95 ms; echo time, 1.07 ms; flip angle, 15 degrees; field of view, 450 x 450 mm; matrix, 256 x 128; and number of excitations = 3. Gadolinium-diethylene triamine pentaacetic acid (Gd-DTPA) or Gd-ethoxybenzyl-DTPA (0.1 mmol/kg, maximum dose not more than 20 mL) was injected intravenously at a rate of 3.0 mL/s using a high-pressure injector (Tennessee XD2003, Ulrich®, Ulm, Germany), followed by a 20-mL saline flush.

By subtracting the pre-contrast image data from the original image data in the venous phase (55, 90, and 120 seconds) using a commercially available software workstation system (Syngo Multimodality Workplace; Siemens®), the background signal could be reduced, allowing the small vessels to be displayed more distinctly. We performed maximum intensity projection rendering and multiplanar reformation separately for the subtracted images to observe the venous system and collateral circulations from all angles in order to assess the relationships among the anatomical structures and adjacent spaces. Furthermore, localized region-of-interest reconstructions were performed to remove shadows from overlapping vessels, thus improving the visualization of target vessels, such as HVs and collateral circulation.

Magnetic resonance and US were performed 1–2 weeks before DSA in all patients. MR-based diagnoses were made by two senior radiologists with considerable experience in abdominal diseases. The readers were blinded from each other's findings and they were also blinded to the results from other images like US and DSA, and when their diagnoses were in agreement, the results were considered valid. HV and IVC lesions were classified as septal obstruction (septum thickness  $\leq 1.0$  cm in HVs and  $\leq 1.5$  cm in the IVC), segmental obstruction (obstruction length  $> 1.0$  cm in HVs and  $> 1.5$  cm in the IVC), and thrombosis or

## MRV Findings of Budd-Chiari Syndrome

completely occluded HV (including cord-like HVs and non-visualized HVs).

### DSA

A Innova-4100 (GE Healthcare®, Milwaukee, WI, USA) digital subtraction angiographic imaging system was used, and a 5F pigtail catheter was placed through the femoral or jugular vein to the edge of the IVC occlusion. Iobitridol (25–35 mL of 300 mg I/mL; Guerbet®, Roissy, France) was injected at a rate of 15–20 mL/s. When the patients presented with a complete IVC occlusion after injection through the femoral vein, a second injection was performed via jugular vein cannulation using a 5F single-curve catheter.

### Classification Criteria for HV and IVC Lesions

Hepatic vein lesions were classified as segmental stenosis, segmental occlusion, membranous stenosis, membranous occlusion, cord-like occlusion or non-visualized. Except for patent IVCs, IVC lesions were classified as segmental occlusion, segmental stenosis, membranous occlusion, membranous stenosis, and hepatomegaly-induced stenosis.

### Membranous Lesions

Membranous lesions were identified as those having a septum thickness  $\leq 1.0$  cm in HVs and  $\leq 1.5$  cm in the IVC (5, 6). The septa of both HVs and the IVC were shown as a transverse or oblique low-signal strip on MRI. Membranous lesions were classified as membranous obstruction or membranous stenosis. There was no blood or contrast medium flowing through the occluded septum in membranous obstructions. For membranous stenosis, blood and contrast medium could be seen passing through the septum on MRI, occasionally with ejection of blood.

### Segmental Lesions

Segmental lesions were identified as obstruction length  $> 1.0$  cm in HVs and  $> 1.5$  cm in the IVC (5, 6). Segmental lesions were also classified as segmental obstruction or segmental stenosis. The lumen and blood disappeared on MRI in the presence of segmental occlusion (Fig. 1). Segmental stenosis was seen as a stenosed lumen with a thickened wall. IVC stenosis caused by compression from an enlarged caudate lobe was not included in the IVC segmental stenosis category (Fig. 2).

### Thrombi

Thrombi in HVs, accessory hepatic veins (AHVs), and

the IVC were seen as diverse intensities in different MR sequences during the development of thrombi. MRI revealed an absence of blood flow in the vessels that were

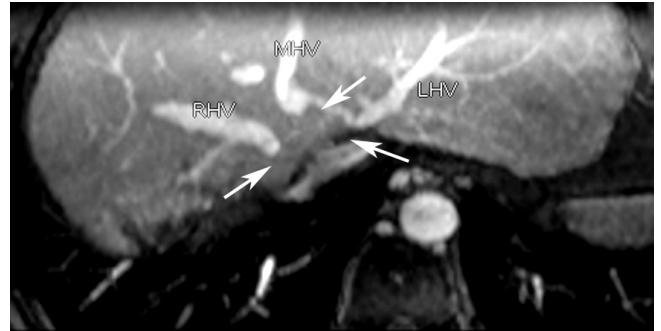


**Fig. 1. Segmental occlusions.** Proximal parts of three HVs show segmental obstruction (arrows), with blood draining through caudate lobe vein. HV = hepatic vein, LHV = left hepatic vein, MHV = middle hepatic vein, RHV = right hepatic vein

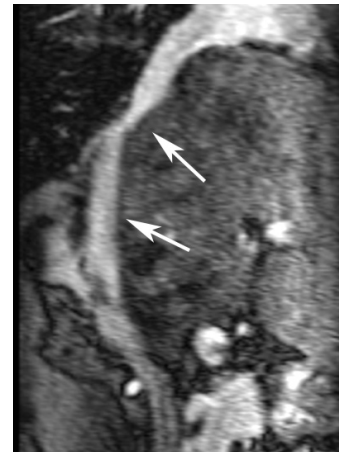


**Fig. 2. Hepatomegaly induced stenosis.** MRV shows intumescent caudate lobe and compressed IVC lumen (arrows). IVC = inferior vena cava, MRV = magnetic resonance venography

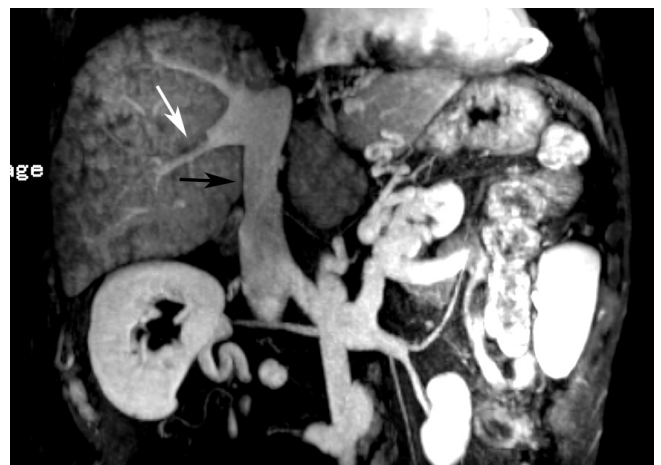


**Fig. 3. Partial thrombosis.** MRV shows blood-filling defects in inferior RHVs (white arrow) and IVC (black arrow), which were partly thrombosed.

completely thrombosed by fresh thrombi. Furthermore, where there was partial embolization, there was a blood-filling defect in the vessel (Fig. 3).

### Cord-Like Occlusion

A cord-like occlusion was identified as complete occlusion of the lumen, which only showed a hypo-intense cord (a persistently thickened wall) on MRI (Fig. 4).

### Non-Visualized

Non-visualized was the term used for cases where no HVs could be identified in their normal anatomic positions.

### Observation of AHVs

The vascular draining conditions were carefully observed if the MRI revealed obstructions in HVs and/or the IVC. The draining branches of the obstructed HVs were mainly AHVs, including the caudate lobe veins and inferior right HVs, certain normal HVs or hepatic subcapsular veins (7). Inferior right HVs are located on the caudal side of the posterior right branch of the portal vein, predominantly in segment VI, and they are situated within the superficial hepatic parenchyma in the renal impression (8, 9). The inferior right HVs enter the IVC at the level of the first portal hilum. Caudate lobe veins are the largest veins draining from the caudate (Spiegel's) lobe and flow directly into the anterior left side, anterior side, or left side of the middle and lower sections of the retrohepatic segment of the IVC (10). All AHVs were identified at confirmable anatomical sites.

### Statistical Analysis

All statistical results were obtained using Excel 9.0

(Microsoft®, Seattle, WA, USA) and SPSS 14.0 (SPSS Inc., Chicago, IL, USA). Descriptive statistics, including the proportion and rate of occurrence of each lesion type, were used to analyze the effectiveness of MRV. Chi-square tests were used to determine significant differences between the two examination methods. Differences showing values of  $p < 0.05$  were considered statistically significant.

## RESULTS

All 52 cases in this group were of chronic BCS and they had HV lesions of varying degrees. Based on the results of DSA examinations, among all patients, 43 (43/52, 83%) had mixed BCS, in which obstructed HVs and an obstructed IVC co-existed in the same patient. No isolated IVC lesions (obstruction in only the IVC) were observed in this study.

Among the 156 total HVs in 52 patients with BCS, there were only 12 patent HVs (2 left HVs, 3 middle HVs, and 7 right HVs) in 12 patients, representing 7.7% of all HVs observed. A total of 144 HVs were obstructed (50 left HVs, 49 middle HVs, and 45 right HVs, with segmental occlusions of the left and middle HVs converging in the trunk in 8 cases), representing 92.3% of all HVs. There were an average of 2.8 (156/52) abnormal HVs per patient. HV lesions were classified as segmental stenosis, segmental occlusion, membranous stenosis, membranous occlusion, cord-like occlusion (the lumen was completely filled with a cord-like occlusion), or non-visualized.

Table 1 shows that occlusive lesions, including cord-like, non-visualized, and segmental occlusions, accounted for the majority of HV lesions. In segmental occlusions, the blood and contrast medium disappeared on MRV (Fig. 1).

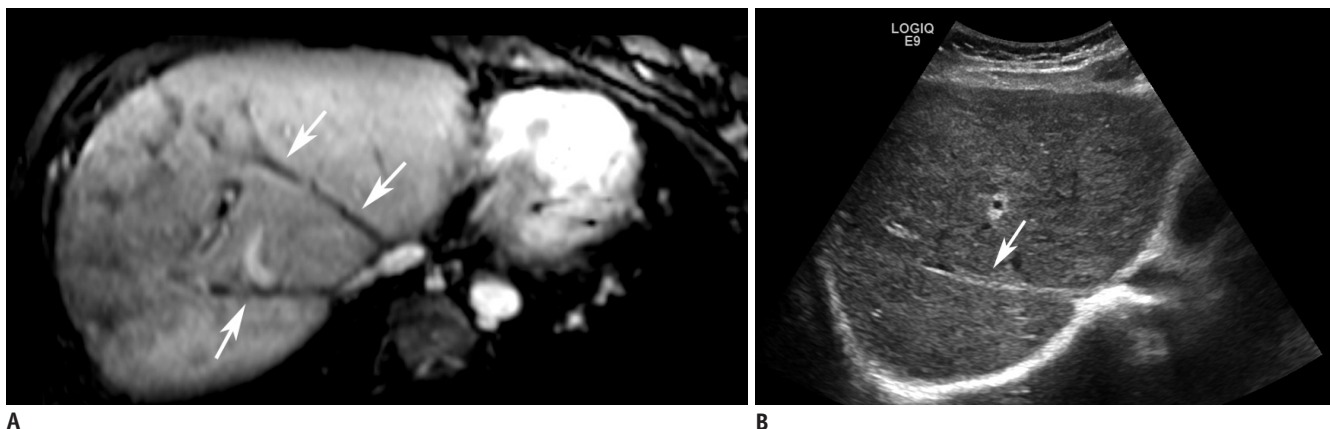


**Fig. 4. Cord-like occlusion.**

**A.** MRV shows hypo-intense cord at original HV anatomic site (arrows). **B.** Ultrasonogram shows HV cord-like occlusion (arrow) in liver parenchyma of same patient.

**Table 1. Number of Each HV Lesion Type Assessed with Magnetic Resonance Venography**

	Cord-Like Occlusion	Non-Visualized	Segmental Occlusion	Segmental Stenosis	Membranous Occlusion	Membranous Stenosis	Segmental Occlusions of Trunks of LHV and MHV
RHV	6	32	5	0	2	0	0
MHV	0	20	21	0	0	0	8*
LHV	0	10	22	6	0	4	8*
Total	6	62	48	6	2	4	16

\*Each of 8 cases with segmental occlusion in trunks of LHV and MHV was counted as 2 obstructed HVs. HV = hepatic vein, LHV = left hepatic vein, MHV = middle hepatic vein, RHV = right hepatic vein

Membranous lesions were primarily membranous stenosis, and they occurred mainly in the left HV. HV membranous stenosis manifested as blood and contrast medium passing through the septum with identifiable jets of blood on MRI; membranous stenosis of the caudate lobe vein showed the same manifestations (Fig. 5). No blood or contrast medium flowed through the occluded septum in cases of membranous obstruction. Cord-like occlusions were observed as hypo-intense cords on MRI, which indicated a completely occluded lumen (Fig. 4). However, MRV was inferior to US in detecting cord-like occlusions (6 vs. 19,  $\chi^2 = 11.077$ ,  $p < 0.001$ ).

Dilated AHVs were well detected in this study, including 50 draining caudate lobe veins (including distinct communicating branches that flowed into them and then drained into the IVC, but excluding tiny, isolated veins without communicating branches) in 36 patients and 37 draining inferior right HVs in 33 patients. Among them, draining caudate lobe veins and inferior right HVs were simultaneously found in 16 patients. MRV revealed that the distal part of the HVs, which were proximally occluded, drained through communicating branches into AHVs and subsequently into the IVC (Fig. 6). There were few proper lesions in draining veins in this group. Two cases showed inferior right HV thrombosis (Fig. 3), 2 cases showed caudate vein membranous stenosis (Fig. 5), and 1 case showed caudate vein membranous occlusion.

Among the IVCs observed, segmental lesions were well visualized with MRV, and segmental occlusions were the most prevalent (Fig. 6A). Membranous lesions included membranous occlusions (Fig. 7) and membranous stenosis. In patients with IVC constriction caused by hepatomegaly, MRV allowed for visualization of not only the compressed IVC lumen but also the intumescent caudate lobe (Fig. 2). The number and type of IVC lesions detected via MRV and DSA are summarized in Table 2.

As shown in Table 2, 7 patients diagnosed with IVC membranous lesions on DSA showed patent IVCs on MRV.



**Fig. 5. Membranous stenosis.** Caudate lobe vein shows membranous stenosis (arrow) with ejecting blood into pouch. CLV = caudate lobe vein

Therefore, we conclude that MRV is inferior to DSA in detecting membranous lesions ( $\chi^2 = 6.125$ ,  $p = 0.013$ ). Except for the identification of membranous lesions, there were no significant differences in detection rates for segmental lesions and thrombosis between MRV and DSA ( $\chi^2 = 0.000$ ,  $p1 = 1.000$ ,  $p2 = 1.000$ ).

## DISCUSSION

Hepatic vein lesions in patients with BCS typically involve more than one lumen and are mixed with IVC lesions, which is consistent with the outcome of the present study. The current MRV detection results showed that damaged HVs account for 92.3% of the total damaged HVs, with an average of 2.8 abnormal HVs per patient, which is in close agreement with our previous research (7). In all HVs, most lesions were occlusive lesions, including cord-like, non-visualized, and segmental occlusions. The most common type of IVC lesion was segmental occlusion. Among the membranous lesions in HVs and the IVC, membranous stenosis was the most common. In membranous stenosis, in addition to a low-signal strip, MRV showed a high-signal ejection of blood in the distal part of the septa, which is

significant for distinguishing membranous stenosis from membranous obstruction. Our research shows that MRV provides high-resolution images that show the extent, level, and form of obstructions situated in the hepatic venous

outflow. This approach has the important advantage of a multi-perspective capacity to observe the spatioanatomic orientation of intra- and extrahepatic vessels, including HVs and AHVs, and collateral circulation from all sides

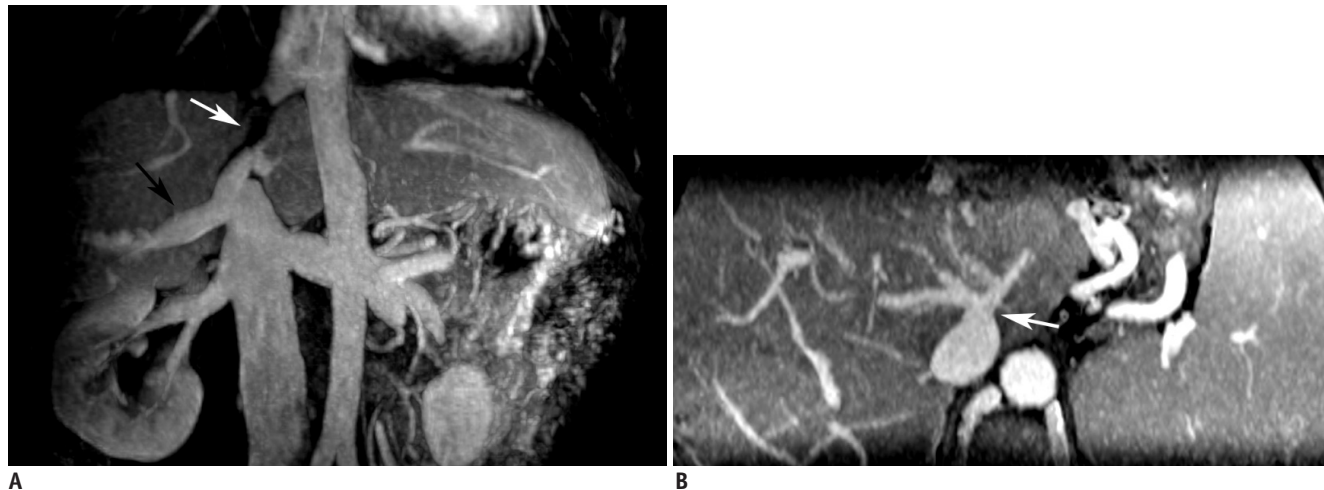


**Fig. 6. Dilated accessory hepatic veins.** Two figures are not same patient. MRV shows segmental occlusion of IVC (white arrow) and dilated inferior right hepatic (black arrow) (A) and caudate lobe veins (B), which drain blood into IVC in third portal of liver.



**Fig. 7. Membranous occlusion.** A. MRV shows membranous occlusion (arrow) of IVC without blood passage. B. Digital subtraction angiography confirms presence of membrane (arrow) shown on angiogram performed through internal jugular and transfemoral veins.

**Table 2. IVC Lesions Detected Via MRI and Comparison with Results of DSA Examinations**

Classification	MRI Examination (n, %)	DSA-Certified Cases (n, %)
Segmental occlusion	24 (3 cases with mixed thrombosis) (46.2)	23 (3 cases with mixed thrombosis) (44.2)
Segmental stenosis	5 (9.6)	5 (9.6)
Membranous occlusion	2 (3.8)	5 (9.6)
Membranous stenosis	5 (9.6)	10 (19.2)
Hepatomegaly-compressed stenosis	7 (13.5)	7 (13.6)
Patent	9 (17.3)	2 (3.8)
Total	52 (100)	52 (100)

DSA = digital subtraction angiography, IVC = inferior vena cava

(11). Moreover, the targeted vessels can be observed in coronal, sagittal, and transverse views with a broad scope of imaging, which can provide more satisfactory images of the vessels.

However, the comparison with US indicates that MRV is less sensitive than US in identifying cord-like occlusions in HVs, which is in accordance with the results of a previous research (12). The reason for this finding is likely related to the different principles of MRV and US. The visualization of veins on MRV scans relies on intraluminal filling with contrast medium. Hemodynamic abnormalities, especially slow blood flow in diseased HVs caused by partial inaccessibility, might be responsible for the difficulty in making MRV-based diagnoses.

Anatomically, in addition to the main blood draining veins, including the left, middle, and right HVs, there is another inferior group of small-diameter HVs that drain blood from the inferior portion of the right and caudal lobes of the liver called AHVs (13). Intrahepatic collaterals between HVs and AHVs or other HVs also exist in people with a normal vascular system. Dilated AHVs can compensatorily drain blood from the obstructed HVs through collateral pathways (14). MRV can satisfactorily display the features and dilation status of caudate veins and inferior right HVs. Therefore, MRV can accurately visualize the draining condition of the HVs and provide beneficial information for making a diagnosis and deciding on the treatment.

Recognizing AHV lesions is also crucial in clinical practice. In addition to the dilated draining AHVs, intrahepatic collaterals connecting obstructed HVs with draining AHVs were found in patients with obstructed HVs. If these patients also show IVC obstruction, AHV dilation could become more severe. At the same time, AHV obstruction causes the rate of blood flow in draining AHVs to slow down, further aggravating hepatic congestion. Our previous study reported that AHV lesions are mainly inferior right HV lesions, including inferior right HV thrombi and segmental stenosis (15). In this group, in addition to the two cases with an inferior right HV thrombus, we observed caudate lobe vein membranous obstruction and membranous stenosis. Furthermore, MRV revealed that the hepatic subcapsular vein ran along the hepatic capsule, and it was more easily visualized than with US.

In this study, proper IVC lesions were classified as segmental obstruction, segmental stenosis, membranous obstruction, or membranous stenosis. Congestive

hepatomegaly due to HV obstruction results in reduced flow in the IVC. IVC stenosis caused by compression from an enlarged caudate lobe does not result from an IVC disease itself; therefore, this entity was excluded from the segmental obstruction category. MRV has a superior visualization capacity in identifying segmental lesions, with a precision of 96.5%, corresponding approximately to that of DSA. Furthermore, because it is noninvasive and does not require the use of radioactive material, MRV could be a better choice for distinguishing segmental lesions in BCS. However, our comparison indicates that MRV was significantly inferior to DSA in visualizing membranous lesions. This finding is likely due to the fact that the spatial resolution of MRV is relatively low; MRV scanning has a scan slice thickness of at least 0.13 cm and an interlayer spacing of at least 0.026 cm.

The intravascular intervention involving percutaneous balloon dilatation angioplasty and stent placement constitutes the main therapeutic modality for BCS (16, 17). Obtaining preoperative imaging to identify the characteristics of lesions is crucial for determining surgical options (18). Patients with membranous obstruction or segmental obstruction with a thickness < 2.0 cm show a satisfactory therapeutic outcome after balloon dilatation angioplasty using an IVC approach (19, 20). However, the therapeutic outcome is related to the thickness of the septum; patients with thick membranes are prone to restenosis. Therefore, based on a previous report (6), we defined a thickness  $\leq 1.5$  cm as membranous obstruction and a thickness > 1.5 cm as segmental obstruction.

All patients with an IVC thrombus showed obstructive lesions above the thrombus, which were mainly completely obstructive. The slow blood flow resulting from IVC obstruction might be responsible for thrombogenesis. Therefore, an IVC thrombus should not be classified as an isolated type; instead, it must be described in detail in the diagnostic report because a fresh thrombus is unstable and likely to become detached, resulting in pulmonary embolism, which is an absolute contraindication for intervention (11).

Magnetic resonance-based IVC examination results were contrasted with the results of DSA. However, in HV examinations, DSA requires the injection of contrast medium into each HV to visualize the lesions, and it usually provides unclear images and causes too much discomfort to the patients; therefore, DSA examinations were not performed as a control for evaluating HVs (21, 22). Additionally, as US

is operator dependent, it is not an accurate control method unless it is being used for evaluating cord-like occlusions; therefore, for other HV lesion types, there is lack of a suitable and accurate method of examination for visualizing the lesions for making a comparison, which is a limitation of this study. Besides, the inclusion of patients with venous occlusion alone is another limitation of our research. We are planning to include an equal number of normal subjects as the control group in our further study.

In summary, this study shows that MRV can display the major features of obstructed HVs and the IVC, which is beneficial for obtaining an accurate diagnosis and implementing appropriate surgical options.

## REFERENCES

- Hefaiiedh R, Cheikh M, Marsaoui L, Ennaifer R, Romdhane H, Ben Nejma H, et al. The Budd-Chiari syndrome. *Tunis Med* 2013;91:376-381
- Hidaka M, Eguchi S. Budd-Chiari syndrome: focus on surgical treatment. *Hepatol Res* 2017;47:142-148
- Klein AS. Management of Budd-Chiari syndrome. *Liver Transpl* 2006;12:S23-S28
- Valla DC. Primary Budd-Chiari syndrome. *J Hepatol* 2009;50:195-203
- Gai YH. [Sonographic classification of blood-drainage in Budd-Chiari syndrome with hepatic vein obstruction]. *Chin J Ultrasonogr* 2008;6:517-520
- Gai YH, Ma S, Guo WB, Liang B, JIA T, Zhang SZ, et al. [Further study of sonographic examination skills and classifications of the inferior vena cava lesions in patients with Budd-Chiari syndrome]. *Chin J Ultrasonogr* 2012;11:965-968
- Gai YH, Cai SF, Guo WB, Zhang CQ, Liang B, Jia T, et al. Sonographic classification of draining pathways of obstructed hepatic veins in Budd-Chiari syndrome. *J Clin Ultrasound* 2014;42:134-142
- Bargalló X, Gilabert R, Nicolau C, García-Pagán JC, Bosch J, Brú C. Sonography of the caudate vein: value in diagnosing Budd-Chiari syndrome. *AJR Am J Roentgenol* 2003;181:1641-1645
- Kanamura T, Murakami G, Hirai I, Hata F, Sato TJ, Kumon M, et al. High dorsal drainage routes of Spiegel's lobe. *J Hepatobiliary Pancreat Surg* 2001;8:549-556
- Xing X, Li H, Liu WG. Clinical studies on inferior right hepatic veins. *Hepatobiliary Pancreat Dis Int* 2007;6:579-584
- Lu X, Yang C, Xu K, Rong YT, Li SD, Li JS, et al. Magnetic resonance venography in the diagnosis of inferior vena cava obstruction in Budd-Chiari syndrome. *Eur Rev Med Pharmacol Sci* 2015;19:256-264
- Faraoun SA, Boudjella Mel A, Debzi N, Afredj N, Guerrache Y, Benidir N, et al. Budd-Chiari syndrome: a prospective analysis of hepatic vein obstruction on ultrasonography, multidetector-row computed tomography and MR imaging. *Abdom Imaging* 2015;40:1500-1509
- Standring S. *Gray's anatomy*, 40th ed. London: Churchill Livingstone, 2008:2108
- Ueda K, Matsui O, Kadoya M, Yoshikawa J, Gabata T, Kawamori Y, et al. CTAP in budd-chiari syndrome: evaluation of intrahepatic portal flow. *Abdom Imaging* 1998;23:304-308
- Cai SF, Gai YH, Ma S, Liang B, Wang GC, Liu QW. Ultrasonographic visualization of accessory hepatic veins and their lesions in Budd-Chiari syndrome. *Ultrasound Med Biol* 2015;41:2091-2098
- Plessier A, Rautou PE, Valla DC. Management of hepatic vascular diseases. *J Hepatol* 2012;56 Suppl 1:S25-S38
- Xue H, Li YC, Shakya P, Palikhe M, Jha RK. The role of intravascular intervention in the management of Budd-Chiari syndrome. *Dig Dis Sci* 2010;55:2659-2663
- Cura M, Haskal Z, Lopera J. Diagnostic and interventional radiology for Budd-Chiari syndrome. *Radiographics* 2009;29:669-681
- Xu PQ, Dang XW. Treatment of membranous Budd-Chiari syndrome: analysis of 480 cases. *Hepatobiliary Pancreat Dis Int* 2004;3:73-76
- Wang ZG. Experience on management of Budd-Chiari syndrome in 143 cases. *Angio Arch* 1989;17:147-152
- Yang C, Li C, Zeng M, Lu X, Li J, Wang J, et al. Non-contrast-enhanced MR angiography in the diagnosis of Budd-Chiari syndrome (BCS) compared with digital subtraction angiography (DSA): preliminary results. *Magn Reson Imaging* 2017;36:7-11
- Shimada K, Isoda H, Okada T, Kamae T, Arizono S, Hirokawa Y, et al. Non-contrast-enhanced hepatic MR angiography: do two-dimensional parallel imaging and short tau inversion recovery methods shorten acquisition time without image quality deterioration? *Eur J Radiol* 2011;77:137-142